Geometrical properties of the potential energy of the soft-sphere binary mixture

Tomás S. Grigera[a)]
Instituto de Investigaciones Fisicoquímicas Teóricas y Aplicadas (INIFTA), Facultad de Ciencias Exactas, Universidad Nacional de La Plata, c.c 16, suc.4, 1900 La Plata, Argentina Facultad de Ingeniería, Universidad Nacional de La Plata, La Plata, Argentina and Consejo Nacional de Investigaciones Científicas y Técnicas (CONICET), Argentina

(Received 12 September 2005; accepted 18 November 2005; published online 9 February 2006)

We report a detailed study of the stationary points (zero-force points) of the potential energy surface (PES) of a model structural glassformer. We compare stationary points found with two different algorithms (eigenvector following and square gradient minimization), and show that the mapping between instantaneous configuration and stationary points defined by those algorithms is as different as to strongly influence the instability index K versus temperature plot, which relevance in analyzing the liquid dynamics is thus questioned. On the other hand, the plot of K versus energy is much less sensitive to the algorithm employed, showing that the energy is the good variable to discuss geometric properties of the PES. We find new evidence of a geometric transition between a minima-dominated phase and a saddle-point-dominated one. We analyze the distances between instantaneous configurations and stationary points, and find that above the glass transition, the system is closer to saddle points than to minima. © *2006 American Institute of Physics*.
[DOI: 10.1063/1.2151899]

I. INTRODUCTION

Interest in the geometric properties of the potential energy surface (PES) of liquids as a mean to understand their dynamics and thermodynamics dates back to the work of Goldstein[1] and Stillinger and Weber.[2] These works showed that to analyze the low temperature dynamics of supercooled liquids and glasses it is useful to map instantaneous configurations (ICs) to the (local) minimum of the PES found directly downhill, called inherent structure (IS). This mapping allows to disregard fast vibrations, focusing on slow, activated, structural relaxations. But if one aims to describe the dynamic crossover taking place around the mode coupling theory (MCT) critical temperature (T_{MC}),[3] the IS mapping is not useful because barriers between minima are no longer relevant at high temperatures and the two time scales cease to be well separated. Within the PES point of view, two approaches have been proposed. One is to consider whole superstructures of minimia (called metabasins[4–6]). Another is to focus on stationary points with some unstable directions: saddle points (SPs).[7]

The latter approach was motivated by results obtained on the p-spin model (a mean field glass model). In this system, a threshold energy exists which separates a low-energy, minima-dominated region, from a high-energy, saddle dominated one.[8,9] The higher the energy, the larger the number K of unstable directions of the typical SP (this number is called the *order*, or *instability index* of the SP, and is equal to the number of negative eigenvalues of the Hessian matrix evaluated at the SP). In this model the average index as a function of the energy of the SP $K(E)$ can be computed.[8] Furthermore, it can be verified directly that at high temperatures the stationary point closer to the typical IC is a SP with extensive K, while it is a minimum ($K=0$) at low temperatures.[10] The dynamic arrest observed at the dynamic transition is related to the fact that the system starts getting trapped, or nearly trapped.[11,12] A similar scenario was then proposed[7] for structural glasses: the glass transformation is the consequence of a geometrical transition. In the saddle-dominated (high energy) phase, the system can relax either by jumping an energy barrier or by finding an unstable direction. In the minima-dominated phase (low energy), the second mechanism is no longer available; as a consequence relaxation times soar. It was shown later that the two-step relaxation observed in the supercooled liquid (and described by MCT) can be qualitatively understood as relaxation in the vicinity of a SP.[13]

This scenario has been explored in several numerical studies of model liquids. Some of these works obtained estimations of the $K(E)$ curve,[14–16] which have been found compatible with the existence of a geometric transition (further evidence for the transition has been found in the context of high frequency vibrations[17]). We stress that the abscissa of the $K(E)$ curve is the energy *of the saddle point*, and not the instantaneous equilibrium energy. Other works have instead studied K as a function of the temperature T,[18–22] showing that K decreases dramatically on approaching T_{MC}. In early studies the view was held that a sharp transition can be observed as a function of temperature, with $K=0$ for $T<T_{MC}$ and $K>0$ for $T>T_{MC}$, but further work has shown[5,21,23] that although K decreases very fast (most likely with an Arrenhius law[5,24]), it is still nonzero for $T<T_{MC}$. This has prompted criticism of the saddle-minima transition point of view (see, e.g., Ref. 24), although a geometric transition, controlled by

a)Electronic mail: tgrigera@inifta.unlp.edu.ar

the energy, is compatible with a smooth $K(T)$ curve (see Sec. IV).

But there is another issue to be discussed when considering $K(T)$ curves. Since the system is never *precisely at a SP*, to define a $K(T)$ curve one needs to introduce a mapping between ICs and SPs (in a sense defining a "basin of attraction" of a SP, and generalizing the IS concept). Additionally, if one wants to somehow interpret dynamic behavior from such curve, the mapping should preserve at least some dynamic information. In analytical studies (e.g., Refs. 10, 25, and 26) ICs are (reasonably) mapped to the nearest SP (using the Euclidean distance or some overlap function). In contrast, in numerical work ICs are mapped to a SP through the algorithm used to find the latter, thus in principle introducing a dependence on the details of the procedure used to find SPs[25,26] and raising the question of the dynamical relevance of the mapping. This is perhaps more worrying given that at least one popular procedure fails rather often, leaving some configurations unmapped (see Ref. 21 and the discussion to follow). Also puzzling are some results[21,22] that seem to indicate that in the typical distance from an instantaneous configuration to a saddle or to a minimum is the same, at variance with the mean field situation.

In this paper we address the issue of the mapping between ICs and SPs, and analyze distances between ICs and SPs and minima in more detail than has been previously done. Our results show that the *K vs T* plots are algorithm-dependent, and that, at least in the soft-sphere model we consider, ICs at high temperature are closer to SPs with $K>0$. The large number of SPs collected allows a new analysis which provides new evidence for the existence of a geometrical transition.

II. MODEL AND ALGORITHMS

We have considered the soft sphere binary mixture,[27,28] which consists of 50% of particles of type A and 50% of type B, interacting with a pair potential $v_{ij}(r)=(\sigma_i+\sigma_j)^{12}/r^{12}$. The radii σ_i are fixed by the conditions $\sigma_B/\sigma_A=1.2$ and $(2\sigma_A)^3+2(\sigma_A+\sigma_B)^3+(2\sigma_B)^3=4$. We have used a system of $N=70$ particles at unit density and a smooth (cubic polynomial) long-range cut-off at $\sqrt{3}$ as in Ref. 16 We have used swap Monte Carlo[29] to equilibrate the system at temperatures $T=1$, 0.683, 0.482, 0.350, 0.260, 0.220. For this system T_{MC} is about 0.24.[16,28] At each temperature, 40 000 equilibrated configurations were saved and used as starting point for minima and saddle point searches. Minima were obtained with Nocedal and Liu's LBFGS algorithm,[30] which code can be obtained from the internet.[31] For SP searches, two different algorithms were employed: square-gradient minimization (SGM) and eigenvector following (EF) (described in the following), to compare two different IC-SP mappings. In all, about $3.2\cdot10^5$ SPs were obtained.

A. Square gradient minimization

One way of finding SPs is minimizing the squared modulus of the gradient,

$$\phi=|\nabla V|^2=\sum_{i=1}^{N}\sum_{\alpha=1}^{3}\left(\frac{\partial V}{\partial x_{i,\alpha}}\right)^2. \tag{1}$$

Since ϕ is non-negative, at the absolute minima $\phi=0$, which implies $\nabla V=0$ (a saddle point). This method is relatively easy to implement, since good numerical minimization algorithms are publicly available (we have used LBFGS[30,31]). The biggest drawback is that minimization can (and does rather often) converge to a *local* minimum, which is neither a saddle point, nor close to one in any reasonable sense.[32]

B. Eigenvector following

This method has been specifically designed to find stationary points of the potential energy. Based on an original proposal by Cerjan and Miller,[33] it has been substantially improved by others (see Ref. 34, and references therein). The problem originally considered[33] was to find a saddle point of index 1 starting from a local minimum of V. The idea was to consider the function on a small sphere around the minimum. Using Lagrange multipliers and a quadratic approximation, one looks for local minima of the function constrained to the sphere. Close enough to the initial point (minimum), there is one local minimum of the constrained function that has higher energy: this is a point along the path that leads to the sought saddle point, and is taken as the starting point of the next iteration. Close to the saddle this criterion no longer applies, so a Newton-Raphson step is taken.

We have used our own implementation of the eigenvector following method as described by Wales and co-workers.[22,35–37] At each iteration a step $\Delta\mathbf{x}$ is proposed, which in the base that (locally) diagonalizes the Hessian is[35,36]

$$\Delta x_\mu=S_\mu\frac{2g_\mu}{|h_\mu|(1+\sqrt{1+4g_\mu^2/h_\mu^2})}, \tag{2}$$

where h_μ are the eigenvalues of the Hessian and g_μ are the components of the gradient in the diagonal base (Δx_μ is set to 0 for the directions where $h_\mu=0$, i.e., uniform displacements). The sign $S_\mu=\pm1$ is chosen as explained in the following. Note that as $g_\mu\to0$,

$$\Delta x_\mu=-\frac{g_\mu}{h_\mu}+O(g_\mu^2),\quad g_\mu\to0, \tag{3}$$

where the first term is the Newton-Raphson step. A set of trust radii $\{\delta_\mu\}$ is mantained (one for each direction).[37] The proposed step is rescaled so that $|\Delta x_\mu|\leq\delta_\mu$ for all μ, and then the position is updated. Initially, the δ_μ are set to 0.2, and at each step are increased (decreased) by a factor 1.2 according to whether the quantity $r=(h_e-h_\mu)/h_\mu$ is less (greater) than 1. h_e is an estimation of the eigenvalue, $h_e=(g_\mu-g'_\mu)/\Delta x'_\mu$, where the prime means the quantity evaluated at the previous iteration.[37]

If $S_\mu=1$, the step increases the energy along the direction μ, thus the algorithm converges to a maximum along this direction. Conversely if $S_\mu=-1$ the algorithm converges to a minimum along μ. Since a saddle point of order K is a maximum along K directions and a minimum along $3N-K$ directions, in princple the algorithm may be made to converge to

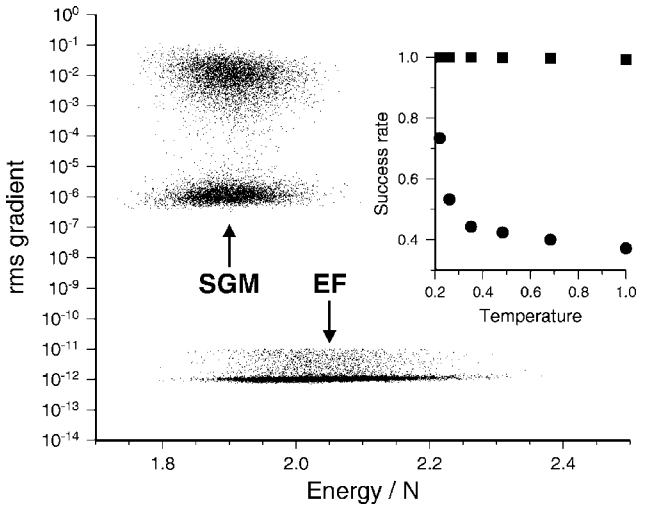

FIG. 1. Root-mean-square gradient vs energy of the configuration obtained with SGM or EF starting from 10 000 equilibrium configurations at $T=0.350$. Inset: success rate (fraction of initial configurations that converge to saddle points) vs temperature (SGM: circles, EF: squares).

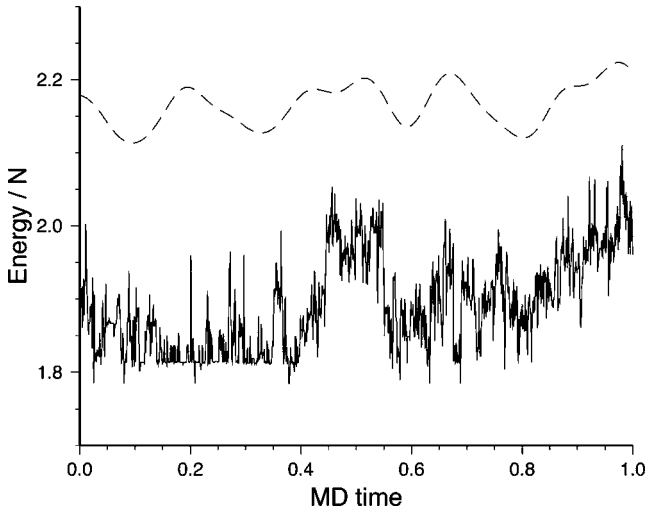

FIG. 2. Instantaneous energy along a 1000-step MD run at $T=0.260$ (dashed-dotted line) and energy of the saddle points found by EF using the MD configurations as starting points (full line). All instantaneous configurations correspond to a single IS.

a saddle of the desired index by setting $S_\mu=-1$ for $1\leqslant\mu\leqslant K$, and $S_\mu=1$ for $\mu>K$. In this work we do not want to fix the index from the start of the search, so for each starting configurations we run 20 steps with $S_\mu=-\mathrm{sgn}\, h_\mu$ and only then fix the index to whatever value it has reached after the first 20 steps.[22]

C. Distances

The distance we report is the Euclidean distance

$$d=\sqrt{\sum_{i,\alpha}(x_{i,\alpha}-y_{i,\alpha})^2}, \tag{4}$$

minimized over the symmetry operations of the system (i.e., translations, the 48 discrete symmetries of the simple cubic lattice, and particle permutations). Minimization over translations is done applying Brent's method[38] (Sec. 10.2) to a distance minimized over the discrete symmetries and permutations. This in turn is found by exhaustive exploration of the discrete symmetries and using the Hungarian algorithm[39] (as implemented by Gerkey[40]) to minimize over permutations.

III. COMPARISON OF SGM AND EF MAPPINGS

A. Basins of attraction and success rate

In Fig. 1 we show the rms gradient $g=\sqrt{\phi/N}$ of the configurations obtained after running SGM and EF on the same set of ICs. EF produces tightly converged saddle points ($g<10^{-11}$), while the configurations found by SGM have rms gradients that cluster around about 10^{-6} and 10^{-2}. To decide whether these configurations are saddle points and compute a success rate (Fig. 1, inset) we have used the SGM configurations as starting points for EF searches and computed the distance between the SGM and corresponding EF converged configurations. In some cases, after a few (3–5) steps, EF found a saddle very close to the SGM configuration (distances of the order of $10^{-5}-10^{-2}$), while in other cases the distance was $O(1)$ or larger (and the number of steps increased). The first case clearly corresponds to an absolute minimum of ϕ, and the second to a local minimum. The criterion we used to accept the SGM configuration as a true saddle was to require that the distance between it and the corresponding EF saddle be less than 0.01. This is approximately equivalent to requiring $g<10^{-4}$ for the SGM configuration.

The high failure rate of the SGM algorithm makes it unsuitable to define basins of attraction of saddle points.[21,22] This failure rate is not due to problems with the minimization algorithm, but to the high number of local minima of the function ϕ.[14,16,21] On the other hand the EF algorithm in principle will always converge to a saddle point (eventual failures being due to numerical problems or implementation details). However, it should be remembered that although basins of attraction for saddle points can be defined using EF, these are not necessarily a reasonable generalization of IS. It is well known that iterative nonlinear algorithms can lead to multiply connected or even fractal basins (a case of fractal basins is the Newton-Raphson algorithm applied to finding the roots of the polynomial z^3-1, see, e.g., Ref. 38 Sec. 9.4). In the case of EF, a detailed study on a three-atom cluster[35] has shown that the basins, though not fractal, are still complex and multiply connected. Their relevance to liquid dynamics is thus not to be taken for granted. We have not performed such detailed analysis here, but in Fig. 2 we plot the instantaneous energy along a short (1000 steps) MD run, along with the energy of the EF saddle points found starting from each IC. All these ICs map to a single IS (minimum). The strong energy fluctuations of the saddles found in this way indicate that the usefulness of the basins of attraction so defined is probably rather limited in understanding the liquid dynamics.

B. Saddle index curves

Let us first consider the saddle index versus temperature curve. In Fig. 3 we plot separately the average value of K for saddles obtained with EF and SGM. We also plot $K(T)$

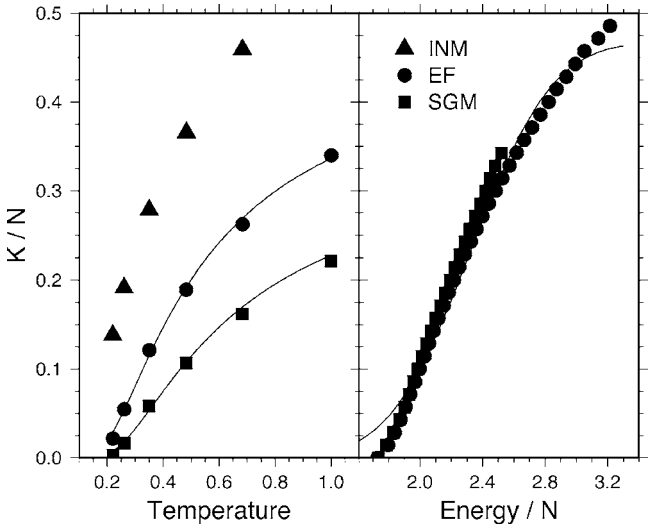

FIG. 3. Average instability index vs temperature (left) and energy (right) for INM, SGM saddles, and EF saddles. Each point is an average over SPs obtained from 40 000 ICs. Lines are fits to the REM expressions (see the text).

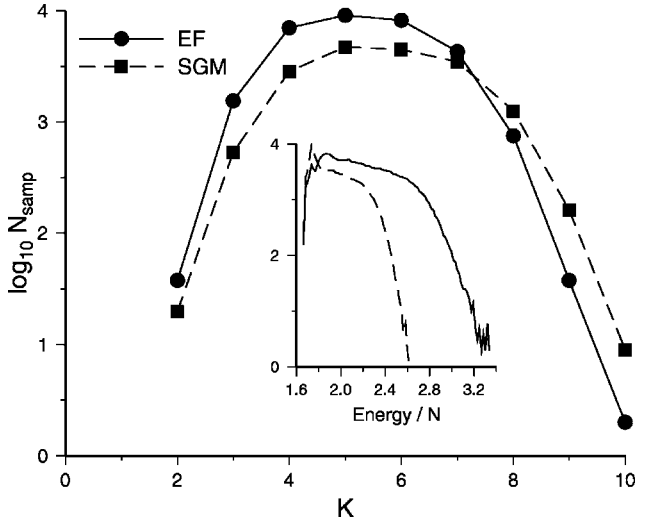

FIG. 4. Logarithm of the number of SPs found vs instability index, for the energy band $1.9 \leqslant e < 2.0$. Inset: Logarithm of the number of SPs vs energy.

evaluated for ICs [the eigenvectors of the Hessian evaluated at an IC are usually called INMs)]. The fact that the curves are algorithm-dependent prevents one from drawing any dynamical conclusion from them, unless there is some reason to expect that the mapping between ICs and SPs preserves some dynamical information. In particular, the critical temperature T_0 where $K(T_0)=0$ (which might or might not be greater than zero) is likely to be algorithm-dependent and thus not of much significance without further evidence of the dynamical relevance of the algorithm chosen to compute $K(T)$.

On the other hand, if we consider K as a function of the *energy* of the saddle point (Fig. 3, right), the curves produced from the SPs collected with EF and SGM are essentially coincident in the region of energies where both algorithms find a significant number of saddles (see inset of Fig. 4). The corresponding curve for INM (not shown) is very close to those corresponding to the SPs, in contrast to what is found in Lennard-Jones.[14] In this purely geometrical plot, the problem of the IC-SP mapping is avoided, and issues such as the existence of a *geometrical* transition can be meaningfully discussed.

Of course, this does not mean one should not worry about possible biases introduced by the algorithms. Indeed, if one considers the SPs within a given energy band, the distribution of the saddle index is slightly different, with EF tending to be slightly narrower (Fig. 4 shows a representative energy band). It is also clear that SGM tends to find SPs with lower energy (inset of Fig. 4). However, we find that the maximum of the $\log N_{\mathrm{samp}}$ vs K curves are the same for both algorithms at all energy bands. The significance of this maximum can be appreciated from the considerations of Sec. IV.

It turns out that one can fit the $K(T)$ curves with the expression given by Keyes *et al.* for the random energy model (REM)[41] (Fig. 3). This model consists of a number of units with fixed ground state energy and excited states with random energies; these units are interpreted as the Adam-Gibbs cooperatively rearranging regions.[42] The expressions are[41]

$$\langle k(e)\rangle = \frac{1}{2}\left[1 - \mathrm{erf}\left(\frac{\epsilon - e}{2\delta}\right)\right], \tag{5}$$

$$\langle k(T)\rangle = \frac{1}{2}\left[1 - \mathrm{erf}\left(\frac{\delta}{2T}\right)\right], \tag{6}$$

where $k=K/N$, $e=E/N$, and ϵ and δ are fit parameters. The $K(T)$ fit is satisfactory within this temperature range if one includes an additional multiplicative fitting parameter A and allows different A and δ for EF and SGM saddles. This is needed for two reasons. First, the REM attempts to model interactions between cooperative regions whose size is unkown, and the value of K we obtain includes eigendirections interior to these regions, which the model does not account for. Second, and more important, the algorithm-dependent IC-SP mapping (which is not an issue in the REM) has to be modeled somehow. On the other hand, the REM $K(E)$ expression is not as successful, even if one allows for different values of A and δ. The discrepancy at low K is to be expected if there is indeed a geometric transition in the soft sphere model (as evidence suggests, see Sec. IV), because Eq. (5) predicts $k(e)>0$ for all e [since $\mathrm{erf}(x)<1$]. Another problem of using the REM to interpret the present data is that the distribution of K at fixed energy is much narrower than the REM prediction, Eq. (18) of Ref. 41 (not shown).

C. Distances

Finally we consider the distances between ICs and the stationary points (IS, EF saddles and SGM saddles) obtained starting from the given IC. The distances reported here are those obtained after minimizing over the symmetries of the Hamiltonian, as discussed in sec. II C. We have found that this distance coincides most of the time with the distance obtained without applying minimizations when one considers an IC and the stationary point obtained from it, so that the

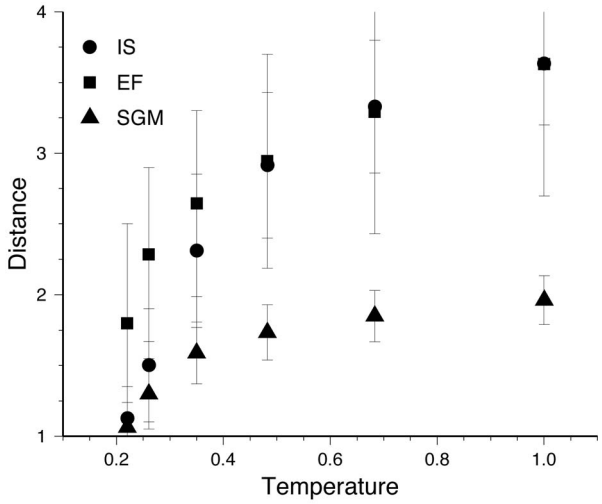

FIG. 5. Average distance from instantaneous configurations vs temperature for minima, EF saddles, and SGM saddles. Error bars are estimates of sample standard deviation (not errors on the averages themselves).

averages we report are not significantly different from those obtained without minimizing. Minimization is however important when computing distances between a configuration and a stationary point obtained from a different IC, as we do in the following.

The average distances as a function of temperature are plotted in Fig. 5. Two things are to be noted: first, SGM saddles are always closer than EF saddles; second, IS are farther than SGM saddles at high temperatures but start to be found closer as temperature is lowered. The first fact points to the influence of the algorithm in defining an IC-SP mapping, stressing the problems of interpretation of $K(T)$ curves. The second provides direct evidence that at high temperatures there is a saddle point to be found closer to the typical IC than the corresponding IS.

To investigate this matter more closely, we look in detail at a short MD trajectory at $T=0.26$, slightly above T_{MC} (Fig. 6). For all ICs in this run, apart from computing the corresponding IS and SGM saddle as usual, we have searched for the nearest SP in the pool of all SPs found at the corresponding temperature. We find again that the system is mostly close to a saddle point of order $K \geqslant 1$, as can be also seen in the inset. This result is natural within the geometrical transition scenario, but this is, to our knowledge, the first direct observation of this fact in a liquid. We furthermore find that the SGM saddle is *not* the closest saddle point. Of course, our procedure does not guarantee to give the closest saddle to a given IC, but we do find SPs closer than the SGM saddle. We must note that Wales and Doyle,[22] in an analysis of a Lennard-Jones binary mixture, did not find differences in the mean distances from ICs to SPs or ISs. It would be interesting to analyze that system at the single configuration level (in the spirit of Fig. 6).

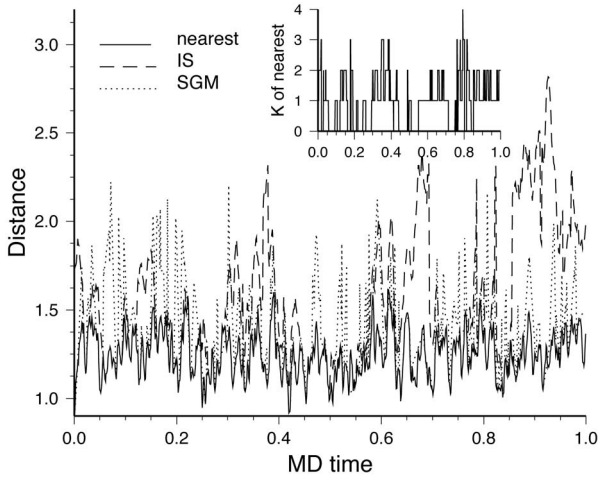

FIG. 6. Distance from instantaneous configurations along a short MD run at $T=0.26$ to the corresponding IS, SGM saddle, and nearest SP found. Inset: index of nearest SP.

IV. SADDLE-MINIMA TRANSITION

Consider the number $\mathcal{N}(K,E)$ of saddle points of order K and energy between E and $E+dE$. For short-range interactions, one expects to be able to divide the system into effectively independent subsystems, so that $\mathcal{N}(K,E)$ should be exponential in the size of the system.[22,43,44] Then $\log \mathcal{N}$ is extensive in the thermodynamic limit, and the complexity $\Sigma(k,e)=(1/N)\log \mathcal{N}(K,E)$ is an intensive quantity. The (intensive) average saddle index can then be written ($e=E/N$)

$$\langle k(e)\rangle = \frac{1}{\mathcal{Z}}\int_0^\infty \frac{K}{N}\exp[N\Sigma(K/N,e)]dK \tag{7}$$

$$= \frac{N}{\mathcal{Z}}\int_0^\infty k\exp[N\Sigma(k,e)]dk, \tag{8}$$

where

$$\mathcal{Z} = \int_0^\infty \exp[N\Sigma(k,e)]dk. \tag{9}$$

Using the saddle point method one gets

$$\langle k(e)\rangle = \hat{k}(e) + O(1/N), \tag{10}$$

where $\hat{k}(e)$ is the point where $\Sigma(k,e)$ attains a maximum (with e fixed), i.e., the solution of $\partial\Sigma(k,e)/\partial k=0$. The saddle-minima transition should be understood as happening at the threshold energy e_{th}, defined as the maximum energy for which $\hat{k}(e)=0$. In the thermodynamic limit this implies $\langle k(e\leqslant e_{\mathrm{th}})\rangle=0$. In finite systems the average will remain positive, but the $\langle k(e)\rangle$ curve will show a fast crossover, remnant of the sharp $N\to\infty$ transition, just as in other thermodynamic phase transitions. Clearly, the transition does not mean that there are no saddles for $e<e_{\mathrm{th}}$ (quite the contrary, there is an exponential number of them), but that they are subdominant respect to minima: $\mathcal{N}(K>0)/\mathcal{N}(0)\to 0$ exponentially with N.

The control parameter of the (geometric) saddle-minima transition is the energy.[7,14–17] If one considers $K(T)$ (assum-

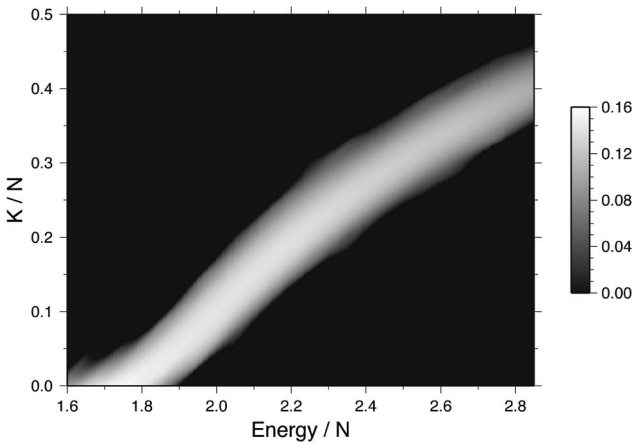

FIG. 7. Logarithm of number of saddle points.

ing one defines a mapping free from the above-discussed problems), one will very likely find $K>0$ below T_{MC} because relaxation processes, though slow, will eventually sample saddle points (transition states). A smooth $K(T)$ curve is thus compatible with a geometric transition. Within the landscape point of view, one can understand the sharp dynamic crossover happening in fragile liquids around T_{MC} as the signature of a geometric transition.[16,17]

Given the large number of SPs obtained for this work (about $3.2\cdot 10^5$), we can try to obtain a rough estimate of the qualitative behavior of $\Sigma(k,e)$. The SPs have been classified into energy bands of width 0.1, and for each band a histogram in K was constructed. The logarithm of the histogram heights gives an estimate of the shape of the actual Σ and is shown in Fig. 7. One can clearly see a maximum that goes to $k=0$ for low values of the energy. From the present data one obtains $e_{\mathrm{th}}=1.77\pm0.01$, which is compatible with the values found in Refs. 16 and 17.

V. CONCLUSIONS

We have shown that in numerical studies of the PES of liquids, the algorithm chosen to associate instantaneous configurations and saddle points can have a significant influence in the analysis of quantities like the saddle index versus temperature curve. Of the two algorithms used, we have found that the saddles found with SGM are closer to the instantaneous configurations than those found with EF. Since no such difference was found in Ref. 22, the present results may reflect a property of the soft-sphere model, or of the present implementation of the EF algorithm. In any case, the point is that curves such as $K(T)$ are not meaningful unless the validity of the IC-SP mapping with respect to dynamic properties is established. It seems that neither of these algorithms is useful to define a particion of phase space into basins of attraction of a SP (in the case of SGM it is rigorously impossible[21]).

The natural variable to analyze geometrical properties of the PES is the energy. We have shown that this choice of variable largely avoids the issue of the IC-SP mapping [in particular the $K(E)$ plot is mostly independent of the mapping], though the algorithms introduce some detectable bias in the sampling. We have produced an estimate of the shape of the saddle complexity that provides new evidence for the existence of a geometric transition in the soft-sphere model.

Finally, our analysis of distances has shown that in this model above T_{MC} the system is closer to saddle points than to inherent structures, as has been shown to be the case in some mean-field models (p-spin,[10] k-trigonometric[25]). We have also found that there are saddles closer than the SGM saddle (this has been explored analytically in the k-trigonometric model, where the SGM saddle was found to be the closest saddle,[25] and the mean-field ϕ^4 model, where it is not[26]).

ACKNOWLEDGMENTS

It is a pleasure to thank A. Cavagna, S. Ciliberti, G. Fabricius, J. R. Grigera, and S. A. Grigera for discussions and suggestions. This work was supported by Consejo Nacional de Investigaciones Científicas y Técnicas, Fundación Antorchas, and Agencia Nacional de Promoción Científica y Tecnológica (Argentina).

[1] M. Goldstein, J. Chem. Phys. **51**, 3728 (1969).
[2] F. H. Stillinger and T. A. Weber, Phys. Rev. A **25**, 978 (1982).
[3] W. Götze and L. Sjørgen, Rep. Prog. Phys. **55**, 241 (1992).
[4] B. Doliwa and A. Heuer, Phys. Rev. E **67**, 030501 (2003).
[5] B. Doliwa and A. Heuer, Phys. Rev. E **67**, 031506 (2003).
[6] R. Aldrin Denny, D. R. Reichman, and J.-P. Bouchaud, Phys. Rev. Lett. **90**, 025503 (2003).
[7] A. Cavagna, Europhys. Lett. **53**, 490 (2001).
[8] A. Cavagna, I. Giardina, and G. Parisi, Phys. Rev. B **57**, 11251 (1998).
[9] A. Cavagna, J. P. Garrahan, and I. Giardina, Phys. Rev. B **61**, 3960 (2000).
[10] A. Cavagna, I. Giardina, and G. Parisi, J. Phys. A **34**, 5317 (2001).
[11] J. Kurchan and L. Laloux, J. Phys. A **29**, 1929 (1996).
[12] S. Franz and M. A. Virasoro, J. Phys. A **33**, 891 (2000).
[13] A. Cavagna, I. Giardina, and T. S. Grigera, J. Phys. A **36**, 10721 (2003).
[14] K. Broderix, K. K. Battacharya, A. Cavagna, A. Zippelius, and I. Giardina, Phys. Rev. Lett. **85**, 5360 (2000).
[15] P. Sha and C. Chakravarty, J. Chem. Phys. **115**, 8784 (2001).
[16] T. S. Grigera, A. Cavagna, I. Giardina, and G. Parisi, Phys. Rev. Lett. **88**, 055502 (2002).
[17] T. S. Grigera, V. Martín-Mayor, G. Parisi, and P. Verrocchio, Nature (London) **422**, 289 (2003).
[18] L. Angelani, R. Di Leonardo, G. Ruocco, A. Scala, and F. Sciortino, Phys. Rev. Lett. **85**, 5356 (2000).
[19] L. Angelani, R. Di Leonardo, G. Parisi, and G. Ruocco, Phys. Rev. Lett. **87**, 055502 (2001).
[20] P. Sha and C. Chakravarty, Phys. Rev. Lett. **88**, 255501 (2002).
[21] J. P. K. Doye and D. J. Wales, J. Chem. Phys. **116**, 3777 (2002).
[22] D. J. Wales and J. P. K. Doye, J. Chem. Phys. **119**, 12409 (2003).
[23] G. Fabricius and D. Stariolo, Phys. Rev. E **66**, 031501 (2002).
[24] L. Berthier and J. P. Garrahan, Phys. Rev. E **68**, 041201 (2003).
[25] F. Zamponi, L. Angelani, L. F. Cugliandolo, J. Kurchan, and G. Ruocco, J. Phys. A **35**, 8565 (2003).
[26] A. Andronico, L. Angelani, G. Ruocco, and F. Zamponi, Phys. Rev. E **70**, 041101 (2004).
[27] B. Bernu, J.-P. Hansen, Y. Hiwatari, and G. Pastore, Phys. Rev. A **36**, 4891 (1987).
[28] J.-L. Barrat, J.-N. Roux, and J.-P. Hansen, Chem. Phys. **149**, 197 (1990).
[29] T. S. Grigera and G. Parisi, Phys. Rev. E **63**, 045102(R) (2001).
[30] D. Liu and J. Nocedal, Math. Program. **45**, 503 (1989).
[31] http://www.netlib.org/opt/index.html.
[32] J. P. K. Doye and D. J. Wales, J. Chem. Phys. **118**, 5263 (2003).
[33] C. J. Cerjan and W. H. Miller, J. Chem. Phys. **75**, 2800 (1981).
[34] D. J. Wales, *Energy Landscapes* (Cambridge University Press, Cambridge, 2004).
[35] D. J. Wales, J. Chem. Soc., Faraday Trans. **89**, 1305 (1993).

[36] D. J. Wales, J. Chem. Phys. **101**, 3750 (1994).
[37] D. J. Wales and T. R. Walsh, J. Chem. Phys. **105**, 6957 (1996).
[38] W. H. Press, S. A. Teukolsky, W. T. Vetterling, and B. P. Flannery, *Numerical Recipes in C* (Cambridge University Press, Cambridge, 1992), 2nd ed.
[39] H. W. Kuhn, Naval Res. Logistics Quart. **2**, 83 (1955).
[40] http://ai.stanford.edu/~gerkey/tools/hungarian.html.
[41] T. Keyes, J. Chowdhary, and J. Kim, Phys. Rev. E **66**, 051110 (2002).
[42] G. Adams and J. H. Gibbs, J. Chem. Phys. **43**, 139 (1965).
[43] M. S. Shell, P. G. Debenedetti, and A. Z. Panagiotopoulos, Phys. Rev. Lett. **92**, 035506 (2004).
[44] Y. V. Fyodorov, Phys. Rev. Lett. **92**, 240601 (2004).